

## BEAM DYNAMICS OF CHINA-ADS LINAC\*

Z.H. Li, F. Yan, J.Y. Tang, H.P. Geng, C. Meng, P. Cheng, B. Sun, Z. Guo, IHEP, Beijing, China

### Abstract

An ADS study program was approved by Chinese Academy of Sciences at 2011, which aims to design and build an ADS demonstration facility with the capability of more than 1000 MW thermal power in about twenty years. The driver linac is defined to be 1.5 GeV in energy, 10 mA in current and in CW operation mode. To meet the extremely high reliability and availability, the linac is designed with much installed margin and fault tolerance. It is composed of two parallel 10-MeV injectors and a main linac. The superconducting acceleration structures are employed except the RFQs. The general considerations and the beam dynamics design of the driver accelerator will be presented.

### INTRODUCTION

China has increased its investment on the nuclear power in the past two decades and this trend is foreseen to be continued in the following decades in order to satisfy the increased energy demands for the economic development. Thus it is more and more urgent to find a solution to transmute the long-lived radioactive wastes produced by the nuclear reactors. A sub-critical system using externally provided additional neutrons is very attractive, it allows maximum transmutation rate while operating in a safe manner. In the beginning 2011, China-ADS project (or C-ADS) was launched in China which will be carried out in three or four phases, with the final goal to develop an ADS demonstration facility with 1000 MW thermal power at 2032. The project is supported financially by the central government and administrated by the Chinese Academy of Sciences. The driver accelerator of 15 MW beam power in the final stage is to be designed and constructed jointly by Institute of High Energy Physics (IHEP) and Institute of Modern Physics (IMP), both under CAS.

Table 1: Specifications for C-ADS Accelerator

Energy	1.5 GeV
Current	10 mA
Beam Power	15 MW
Frequency	(162.5)325/650MHz
Duty factor	100%
Beam loss	<1 W/m
Beam Trips/Year[1]	<25000 1s<t<10s <2500 10s<t<5min <25 t>5min

As the key part of the C-ADS facility, the driver accelerator is a CW proton linac of very high beam power. It uses superconducting acceleration structures except the

\* Work supported by NSFC (10875099, 91126003), the China ADS Project (XDA03020000), IHEP special funding (Y0515550U1) #lizhahui@ihep.ac.cn

RFQs. The design specifications for the proton beam are shown in Table 1. For the first phase, the project goal is to build a CW proton linac of 50 MeV and 10 mA by about 2015. The first phase itself will be executed progressively in several steps, with the first step to build two 5-MeV test stands of different designs by IHEP and IMP in parallel.

The C-ADS linac of 15 MW in beam power is far beyond the capability of the existing proton linacs. The 10-mA beam current looks not so ambitious compared with the existing pulsed machines, but the required beam loss level of  $10^{-8}$ /m at high energy asks for a very delicate dynamics design. Furthermore, the CW operation will give even more difficulties. In order to avoid the risk of thermal problems, superconducting structures are applied from very low energy (3-5 MeV), which will introduce further difficulties in dynamics design. Besides these, the very stringent requirements on beam trips are believed to be potential “show stopper” for the ADS project and need to be considered at the very beginning of the design, and special measures have to be taken to satisfy these requirements.

### DESIGN PHILOSOPHY AND GENERAL LAYOUT

For the C-ADS, the linac has very high beam power and very high reliability that is not possessed by any of the existing linacs. This requires special design strategies to be integrated at the beginning of the design.

#### *Fault Tolerant Design [2]*

For an ADS application, any beam trip lasting more than a few seconds will be considered as a major accelerator failure, possibly leading to the reactor core cool-down. Thus, the philosophy prevailing on current pulsed machines to cope with component failures should be reconsidered. In particular, for each failure analysis, the design should look at the ability to either maintain the beam under safe conditions, or to recover the beam through, in less than several seconds. This requirement appears to be highly challenging, given the state-of-the-art in the accelerator reliability. It is clear that suitable design strategies have to be followed early in the conceptual design stage. The main guidelines are: a strong design (which makes extensive use of component derating and proper redundancy) and a high degree of fault tolerance (i.e. the capability to maintain beam operation within nominal conditions under a wide variety of accelerator component faults) by means of local compensation or hot spare.

It is the common knowledge that any main component failure at low energy is difficult to be compensated by adjusting neighbouring elements so that large beam loss will happen in the downstream linac. At the C-ADS, we

also adopt the design with two identical injectors of 10 MeV, so one can be the hot-spare of the other [3]. Two different injector schemes are under developing, as shown in Figure 1.

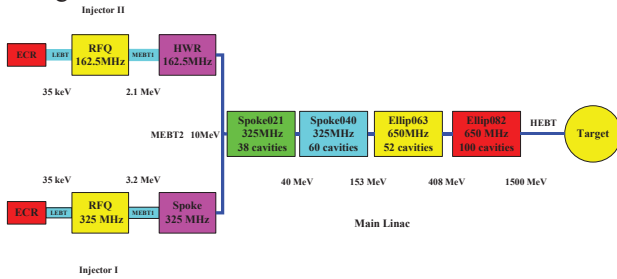


Figure 1: Layout of the C-ADS driver linac with two different injector schemes.

In the main linac section, a fully modular superconducting linac brings the beam up to the final energy with spoke and elliptical cavities. This section is designed to be intrinsically fault tolerant, which means that an individual cavity or focusing element failure can be handled at all stages without introducing significant beam loss along the linac by means of local compensation-rematch method. The local compensation – rematch methods for different element failures are studied systematically [4], it shows that with proper compensation and re-matching, the beam can be accelerated to the final energy without serious beam quality de-rating in the cases of cavity, solenoid and quadrupole failures.

### Superconducting Cavities

Normal conducting acceleration structures have a good foundation in industry fabrication compared with superconducting ones and are widely used in pulsed machines, especially at low energy range. But for CW machines, very high thermal deposit in copper cavities is very hard to deal with, and a linac based on normal conducting structures of many acceleration gaps is not fault tolerant. Therefore, it becomes evident that the C-ADS linac adopts superconducting structures from very low energy.

After the optimization of the acceleration efficiency and cavity types, two types of single-spoke cavities working at 325 MHz with geometry betas of 0.21 and 0.40, and two types of 650-MHz 5-cell elliptical cavities with geometry betas of 0.63 and 0.82 are applied for the

main linac. Considering the requirement in high reliability, the cavities will work at conserved state. The maximum surface electric and magnetic field for spoke cavities are set at 32.5 MV/m and 65 mT, respectively, and the values for the elliptical cavities are 39 MV/m and 65 mT. In addition, 30% of the cavity capability is reserved for local compensation, and this is derived from the fact that four cavities are needed with the local compensation rematch method when one cavity failure happens. The parameters of the cavities are listed in Table 2.

Table 2: Main Parameters of the Superconducting RF Cavities in the C-ADS Linac

Cavity type	$\beta_g$	Freq. MHz	Vmax MV	Emax MV/m	Bmax mT
Single Spoke	0.12	325	0.82	32.5	47.5
Single Spoke	0.21	325	1.64	31.14	65
Single Spoke	0.40	325	2.86	32.06	65
5-cell elliptical	0.63	650	10.26	37.72	65
5-cell elliptical	0.82	650	15.63	35.80	65

### Lattice Structures

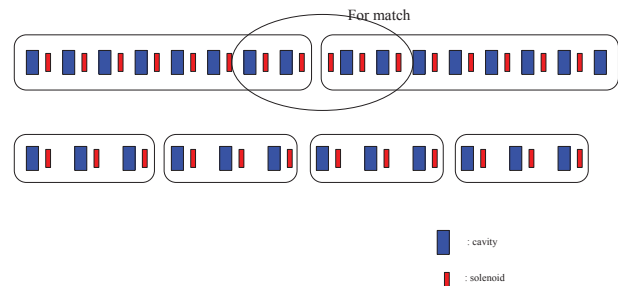


Figure 2: Compact and strictly periodic lattice structures (upper: compact; lower: periodic).

As mentioned in the previous section, the main linac needs to be intrinsically fault tolerant. Besides the derating cavities and redundancy design, the lattice structure is also very important to achieve fault tolerant design.

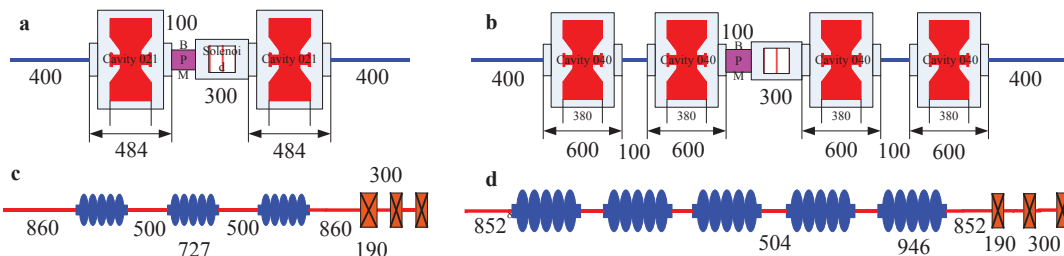


Figure 3: Lattice structures of main linac (a: Spoke021 section; b: Spoke040 section; c: Ellip063 section; d: Ellip082 section).

The lattice structure for the main linac can be classified as compact and strictly periodic types as shown in Figure 2. The compact one is widely used in heavy ion machines [5], it is characterised by relatively short period lengths, and the segmentation between two cryomodules is realized by missing one cavity or solenoid. With this kind of lattice structure, the cavities and solenoids adjacent to the segmentation point will be set quite differently from the others; the failure of these elements will have more impact on the beams. Furthermore, this kind of lattice structure will introduce more points with discontinuity of focusing strength and special matching procedures need to be performed at these points, which will increase the chances of introducing mismatch.

On the contrary, the periodic lattice structure has no problem at cryogenic segmentations. The matching is only needed at the conjunctions of different sections. The C-ADS main linac has adopted periodic lattice for all the superconducting sections as shown in Figure 3.

### Injector Schemes

The front end of a proton linac is usually composed of ion source, LEPT, RFQ and MEPT. Great improvements in RFQ have been made since its invention; however, the RFQ technique with a stable CW operation still needs to be proven. The thermal management is believed to be one of the risks which threaten the steady operation of the RFQ in CW mode. The most effective way to alleviate this risk is to decrease the surface power density at the electrodes, such as by increasing the electrodes area by lowering the operation frequency, the lower inter-vane voltage and so on. Two technical approaches for the injector using 325 MHz and 162.5 MHz, respectively, are under development at IHEP and IMP in parallel.

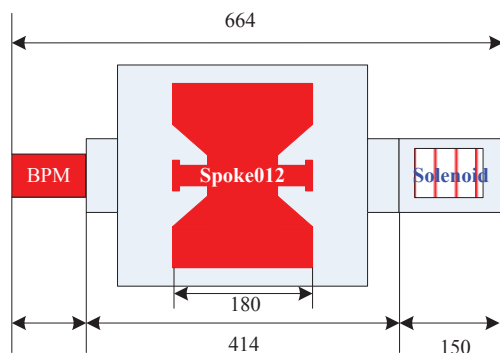


Figure 4: Unit cell of the spoke012 section.

For the Injector-I scheme, a 325-MHz, 3.2-MeV, 4-Vane RFQ has been designed and is under fabrication. The inter-vane voltage is 55 kV, much smaller than the popular design, aiming to decrease the power density to a safe level. The injection energy of 35 kV is helpful in obtaining a relatively smaller output longitudinal emittance (0.16 mm.mrad in normalized rms), about 0.8

times the transverse one. The small longitudinal emittance is found very useful in designing the downstream superconducting sections. Then a 2.06-m long MEPT (MEPT1) [6] is followed. It is mainly composed of two bunchers, six quadrupoles and beam instrument devices. It is employed to match and transfer the beam to the superconducting section of Injector I.

The superconducting section of Injector-I has one 9-m long cryomodule with twelve single spoke cavities [7] and eleven solenoids inside, it will accelerate the beam to 10 MeV. The unit cell of the lattice is shown in Figure 4.

The geometry beta of the cavity is only 0.12 which is considered very small, and it increases the difficulty of developing the cavity. The compact lattice with short solenoid (150 mm) and larger absolute synchronous phase (-46~-30 degrees) is applied to improve the longitudinal beam dynamics. The evolution of the normalized RMS emittance along Injector-I is plotted in Figure 5.

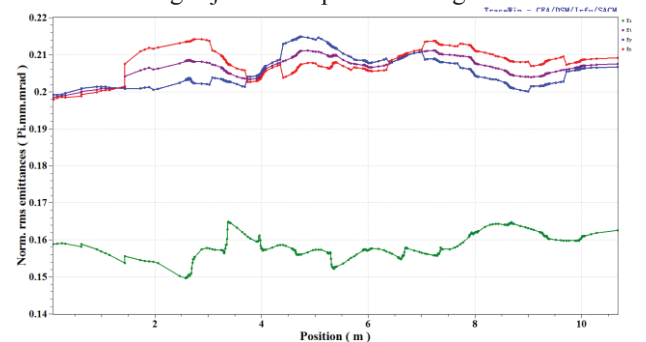


Figure 5: Normalized RMS emittance along Injector I (MEPT1 and Spoke021 section).

For the Injector-II scheme, a 162.5-MHz, 2.1-MeV, 4-Vane RFQ and a superconducting section based on 162.5-MHz HWR cavities has been designed. The details can be found in the references [8].

As the first step, two 5-MeV test stands based on the two different technical solutions are under construction. We will make decision for the injector scheme based on the performance of the two test stands.

### BEAM DYNAMICS DESIGN

In order to allow hands-on maintenance, it is generally required that the maximum allowed beam loss rate along a high power proton linac should be lower than 1 W/m. From beam dynamics point of view, the corresponding particle loss rate needs to be controlled less than  $10^{-8}/\text{m}$  at high energy part, which poses a great challenge in beam dynamics design.

#### ynamics Criteria

The following criteria [9] are followed in the C-ADS beam dynamics design.

- Keeping the zero current phase advance per period in both longitudinal and transverse phase planes below 90 degrees.

- Keeping the external focusing forces changing smoothly and continually.
- Special care to be taken to avoid the parametric resonance as well as space charge resonances.
- Enough acceptances in the phase planes.

Even with a relatively low beam current of 10 mA at C-ADS, the relatively long period length makes the focusing is rather weak compared with the cases using normal conducting DTL. The tune depression along the main linac is only about 0.75 as shown in Figure 6, so the space charge effect is still quite strong and the envelope instability should be taken into account. Furthermore, we find that the smooth approximation is no longer valid at the low energy part since the period length is much larger than the effective length of the cavity, which may produce parametric resonance and cause halo formation. This parametric resonance can be avoided if the phase advance per period is below  $90^\circ$ .

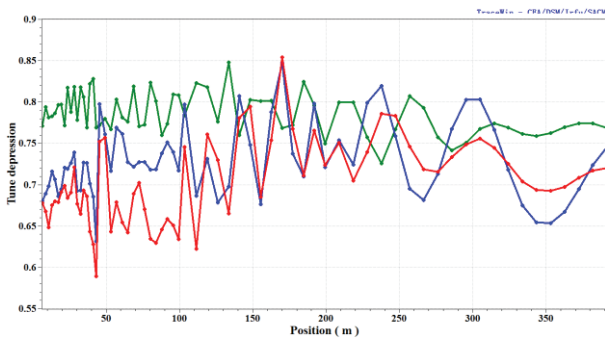


Figure 6: Tune depression along the main linac (Green:  $z$ , blue:  $x$ , red:  $y$ ).

### Design Procedures

The superconducting sections of C-ADS linac can be designed with the following steps.

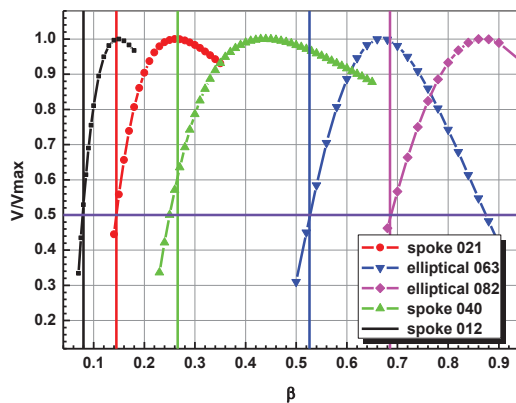


Figure 7: Acceleration efficiency along the C-ADS linac.

First, the cavity types and the energy range of each cavity should be determined, which is the foundation of the cavity optimization. The transition time factor (TTF) of the cavities in  $\pi$ -mode can be calculated analytically [10]. The effective energy range of each cavity type is not symmetrically centred at the optimum beta, but shifted to lower energy. The smallest effective acceleration

efficiency is about 0.5. Figure 7 shows the effective acceleration efficiency for the C-ADS linac.

Secondly, the electromagnetic design of the cavities will be performed and the three-dimensional electromagnetic field distributions can be extracted. With the field distributions and geometries of cavities, transverse focusing elements and other accessories, the lattice can be constructed. The field levels and synchronous phases of the cavities, and the magnetic fields of the focusing elements should be optimized to follow the design criteria. The working point is selected to be in resonance-free region in the Hofmann Chart [11] and to approximately obey the equipartitioning condition [12]. Then the matched beam parameters can be founded with multi-particle simulations by using standard input beam distributions such as 6D waterbag distribution. In this step, the continuity of the zero-current phase advance per meter should be maintained at the junction of two adjacent sections by optimizing the period length, the cavity phases and field levels, and the number of cavities in one period. Of course, the beam parameters, such as RMS emittance and halo parameters should also be optimized to an acceptable level.

Then after, the matching between sections should be performed. The match is usually realized by varying the synchronous phases of cavities and the focusing strengths of the transverse focusing elements around the junction of sections. The synchronous phase should be optimized to move towards more negative so that the acceptance does not decrease dramatically. After this step, the baseline of the linac lattice can be achieved and the beam dynamics should have a good performance. For example, the RMS envelopes should change smoothly, the RMS emittance growth should be kept below 10% and so on.

At last, error studies and closed orbit corrections should be performed, which will verify if the design can meet our design goals in more realistic conditions. Based on the error analysis, the error specifications for the hardware and installation alignments will be determined with iterations with hardware engineering designs.

The C-ADS linac has been designed by following the above procedures. It can be divided into three major sections: Injectors, Main linac [13] and MEBT2 [14]. MEBT2 is very critical in connecting two injectors to the main linac. For each part, the multi particle simulation results are quite promising: the growth in the RMS emittance is less than 10%, the particle distribution is not distorted and no severe beam halo is produced. With proper close orbit correction scheme, no particle loss is found even with errors included [15].

### END TO END SIMULATIONS

End to end simulations for the C-ADS linac are performed based on the design of each part. The multi-particle simulations in the RFQ are performed with PARMTEQM, and the initial particle distribution is water-bag in the transverse plane and uniform in the longitudinal plane with total number of 100000. The

output is used as the initial distribution for the following sections. Figure 8 shows the initial particle distribution at the RFQ exit.

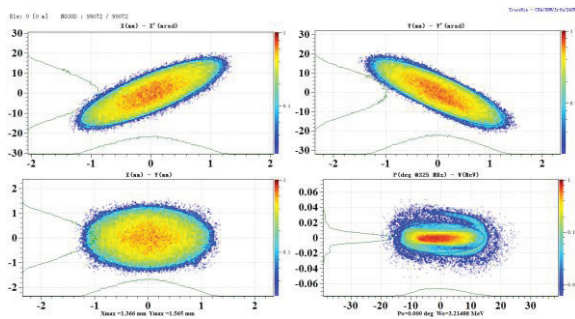


Figure 8: Particle distributions at the RFQ exit.

TraceWin is used to track beams through the downstream sections, and the beam envelopes in the three directions are plotted in Figure 9.

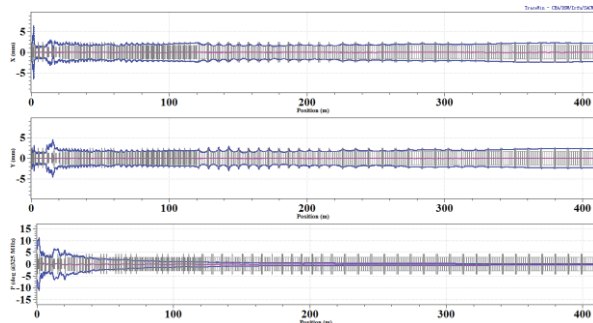


Figure 9: RMS envelopes along the C-ADS linac.

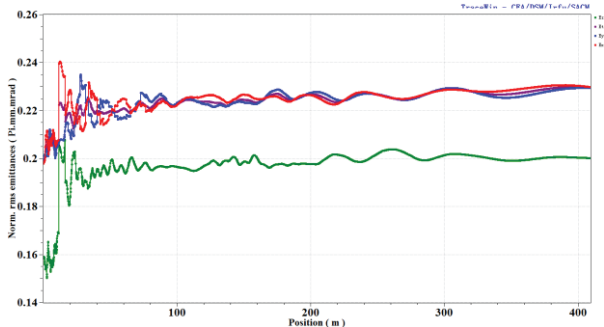


Figure 10: Normalized RMS emittance along the linac.

The RMS envelopes in the transverse directions are quite smooth, but at the beginning of the Spoke021 section, the oscillation in the longitudinal direction is observed, which indicates the possible mismatch between MEBT2 and the Spoke021 section. Figure 10 gives the evolution of the normalized RMS emittance along the linac and a significant growth in the longitudinal RMS emittance can be found in the beginning of the Spoke021 section. Though there is no particle loss, evident beam halo at the exit of the linac can be found, as shown in Figure 11, which indicates that the design is not as robust as required. With errors included, about  $6 \times 10^{-8}$  particles are lost. In the future, the matchings between the sections should be reoptimized with this more-or-less realistic

distribution, and further design optimizations are also needed.

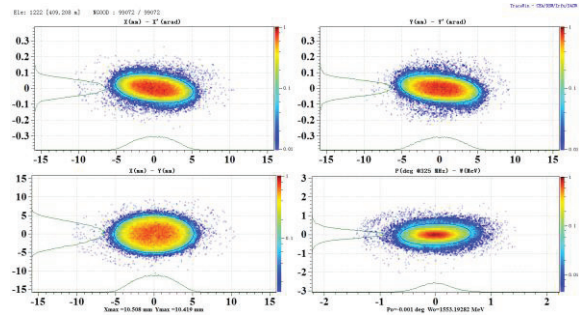


Figure 11: Particle distributions at the exit of the linac.

### CONCLUSIONS

A self-consistent accelerator physics design of the C-ADS linac is obtained, which meets the very strict requirements for ADS applications. At present, the matching between the injectors and the main linac is still not perfect and the optimization of the MEBT2 needs to be studied further. The optimization of the beam dynamics in the RFQ for a good longitudinal distribution will also continue.

### REFERENCES

- [1] R.L. Sheffield, "Utilization of accelerator for transmutation and energy production", HB2010, Morschach, Switzerland, 2010, p1.
- [2] J-L.Biarrotte, Preliminary design studies of an experimental Accelerator-Driven System, XADS-DEL04-063, 2004.
- [3] J-L. Biarrotte, "Beam Dynamics Studies for Fault Tolerance Assesement of the PDS-XADS Linac Design", EPAC2004, Lucerne, Switzerland, p. 1282.
- [4] B. Sun et al., "Compensation-rematch for major element failures in the C-ADS accelerator", MOP220, these proceedings.
- [5] P.N. Ostroumov, J. of physics, Vol.59, No. 6, December 2002, p895.
- [6] H.Geng et al., "The MEBT Design for the China Accelerator Driven System", IPAC'11, San Sebastian, Spain, p.2604.
- [7] LI Han et al., "Design study on very low Beta spoke cavity for China-ADS", Chinese Physics C, V.36, 2012, p.761.
- [8] Y.He et al., "The Conceptual Design of Injector II of ADS in China", IPAC'11, San Sebastian, Spain, p.2613.
- [9] F.Gerigk, "Space Charge and Beam Halos in Proton Linacs", Proc. of the 2002 Joint USPAS-CAS-Japan-Russia Accelerator School, 2002, p257.
- [10] P.N. Ostromov, New Journal of Physics, 8(2006), p281.
- [11] I. Hofmann and O.Boine-Frankenheim, Physical Review Letters, V87 (3), 034802.
- [12] M. Reiser and N. Brown, Physical Review Letters, 1995, Vol. 74, No. 7, p1111.
- [13] F. Yan et al., "Physics Design of the C-ADS Main Linac with Two Different Injector Schemes", MOP221, these proceedings.
- [14] Zhen Guo et al., "The MEBT2 Design for the C-ADS", MOP217, these proceedings.
- [15] C. Meng et al., "Error Analysis and Correction Scheme in C-ADS Injector-I", MOP219, these proceedings.